Angle-resolved photoelectron spectroscopy of the core levels of N2O

M. Schmidbauer, A. L. D. Kilcoyne, K. J. Randall, J. Feldhaus, A. M. Bradshaw, M. Braunstein, and V. McKoy

Citation: The Journal of Chemical Physics **94**, 5299 (1991); doi: 10.1063/1.460514
View online: http://dx.doi.org/10.1063/1.460514
View Table of Contents: http://scitation.aip.org/content/aip/journal/jcp/94/8?ver=pdfcov
Published by the AIP Publishing

Angle-resolved photoelectron spectroscopy of the core levels of N_2O

M. Schmidbauer, A. L. D. Kilcoyne, K. J. Randall, J. Feldhaus, and A. M. Bradshaw
Fritz-Haber-Institut der Max-Planck Gesellschaft, Faradayweg 4-6, D-1000 Berlin 33 Germany

M. Braunstein[a] and V. McKoy
Arthur Amos Noyes Laboratory of Chemical Physics, California Institute of Technology, Pasadena, California 91125

(Received 11 December 1990; accepted 4 January 1991)

We have measured photoionization cross sections and photoelectron asymmetry parameters for each of the core levels of N_2O. We have also carried out frozen- and relaxed-core Hartree–Fock studies of these cross sections so as to better understand the underlying shape resonant structure and the role of electronic relaxation in these processes. A broad shape resonance is observed in each of the core-hole cross sections at 10-20 eV kinetic energy and there is some evidence of a second shape resonance near the thresholds, an energy region which is not accessible experimentally. The cross sections also exhibit site-specific behavior with maxima at widely separated photoelectron kinetic energies. These differences probably arise from the fact that photoelectron matrix elements for different core orbitals probe different regions of the shape resonant orbital which extends over the entire molecule. Although the higher energy shape resonances appear quite similar, Hartree–Fock studies show that the central nitrogen resonance is more sensitive to effects of electronic relaxation than the terminal nitrogen or oxygen resonances. Large differences are also seen between the photoelectron asymmetry parameters for the central and terminal atoms.

I. INTRODUCTION

The general properties of shape resonances in photoionization are fairly well understood from numerous studies on diatomics and other small molecules.[1] However, one of the key questions for larger molecules, where several resonances can be present in the continuum, is to what extent a shape resonance can be viewed as spatially localized between particular nuclei (and thus attributed to specific bonds). Nitrous oxide, a linear molecule with the configuration N–N–O, is a prototypical example for the study of shape resonances since it bridges the gap between simple diatomics and polyatomic molecules.[2–7] The question of localization of shape resonances in N_2O has recently been addressed in combined experimental and theoretical, vibrationally resolved studies of 7σ photoionization leading to the $A\,^2\Sigma^+$ state of N_2O^+.[4–6] Here, the presence of a σ shape resonance located 3–5 eV above the 7σ ionization threshold was seen to give rise to strong non-Franck–Condon behavior. The distinctly different behavior of the symmetric and antisymmetric stretch vibrational modes seen in the fluorescence[5] and photoelectron[6] experiments and in theoretical studies[4] of these spectra, clearly show that this resonance spatially extends over the entire molecule and is not simply characteristic of the N–N or the N–O bond. In addition, a second, weaker shape resonance about 15–20 eV above the 7σ threshold is evident in the experimentally determined asymmetry parameter[2] as well as in multiple scattering $(MSX\alpha)$[2] and in frozen-core Hartree–Fock (FCHF) calculations.[3] The same is true for the isoelectronic molecule CO_2, where two shape resonances are also observed in photoionization studies.[8] The observation of more than one shape resonance in a single partial channel may perhaps be quite normal in the photoelectron spectra of polyatomic molecules.[9–11]

On going from valence to core excitation the continuum resonances usually shift a little (1–4 eV) towards lower kinetic energy due to differences in screening between localized and delocalized holes.[1] There is, indeed, clear experimental evidence of shape resonances above the nitrogen and oxygen K edges of N_2O around 424 and 555 eV, respectively, in the total photoabsorption cross section curves.[12,13] This would be consistent with a small shift to lower photoelectron energy of the weak shape resonance seen at higher energy in valence shell studies of N_2O.[2–6] In contrast to the valence levels, vibrationally resolved photoelectron spectroscopy on the core levels of gas phase samples is not yet feasible since high-resolution monochromators with sufficient photon flux are not available. However, in the case of N_2O one can still probe the continuum resonances from all nuclear sites selectively and thus obtain valuable information: The anisotropic molecular potential gives rise to a large chemical shift of 4 eV between the ionization energies (IE) of the N 1s electrons. The values of the IEs are 408.5, 412.5, and 541.2 eV for the terminal nitrogen (N_T), the central nitrogen (N_C), and the oxygen atom, respectively.[14] Site-specific studies of these N–core levels therefore require only moderate energy resolution and can be performed on existing monochromators. Recently, partial photoionization cross sections and their associated asymmetry parameters for the ionization of the different core electrons of N_2O have been measured and calculated by Grimm *et al.*[7] using the continuum

[a]Present address: T-12 Division, Mail Stop B-268, Los Alamos National Laboratory, Los Alamos, New Mexico 87545.

 0021-9606/91/085299-07$03.00

MSXα method. This study shows that a σ shape resonance, seen in ionization from the 7σ orbital, is also evident in 1*s* ionization. The shapes of the partial cross section and β parameter curves are found to depend on the specific atomic site from which the core electron is ionized. The agreement between theory and experiment in this study is generally good. However, large scatter in the data, due to low photon intensity, and a restricted energy range precluded a detailed comparison with theory. We have therefore measured the *K*-shell photoionization cross sections of N_2O with much higher intensities and lower statistical errors and report here an angle-resolved photoelectron study down to a few eV above threshold. We also report calculations in both the frozen-core Hartree–Fock (FCHF) and relaxed-core Hartree–Fock (RCHF) approximations so as to more fully understand the origin of site-specific differences seen in these shape resonances.

In the next section we briefly describe the experiment and outline our data analysis procedure. In Sec. III we outline the procedures used in our Hartree–Fock level calculations of the photoionization cross sections and photoelectron angular distributions. In Sec. IV we present and discuss our experimental cross sections and asymmetry parameters and compare them with theoretical results obtained from MSXα, FCHF, and RCHF calculations.

II. EXPERIMENT

Angle-resolved photoelectron spectra were recorded using a cylindrical mirror analyzer (CMA) with its axis collinear with the synchrotron light beam. The electron collection angle is 54.7° relative to the axis, corresponding to the photoelectron "magic angle," rather than to the more usual CMA value of 42.3°. Thus on integrating 2π around the axis, the measured intensities are directly proportional to the cross section and are independent of the degree of polarization of the light and of the angular distribution of the photoelectrons.[15] In addition, point-to-ring focusing is used in the CMA. Hence by utilizing a multichannel-plate detector and an eightfold segmented anode, eight photoelectron spectra in different spatially symmetric directions can be recorded simultaneously, allowing the determination of the asymmetry parameter of each spectral line from the intensity variation between these segments. A more detailed description of the apparatus will be published elsewhere.[16]

All spectra have been recorded with a constant CMA pass energy (80 eV for the nitrogen, 100 eV for the oxygen spectra). The transmission of the instrument has been determined with the same monochromator from carbon 1*s* photoelectron spectra of CO and argon 2*p* spectra, whose cross sections and β parameters are fairly well known.[17–20] However, at the lower kinetic energies there are certain discrepancies between the CO- and argon-derived transmission curves which limit the accuracy near threshold. The intensity and the degree of polarization of the monochromatic synchrotron light have been determined from neon 2*s* and 2*p* measurements using the cross sections and β parameters of Wuilleumier.[21] The nitrous oxide was obtained commercially with a purity of 99.0%, the residual

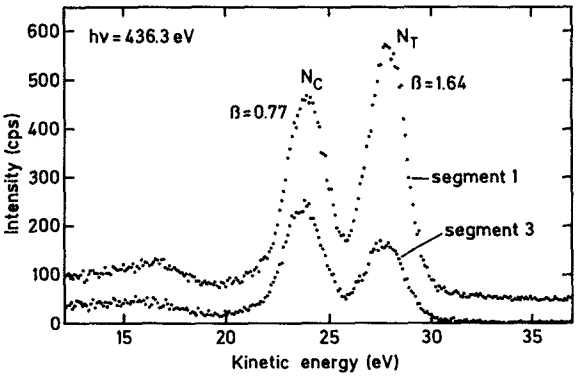

FIG. 1. Photoelectron spectra collected on anode segments 1 and 3 (see the text) at 436.3 eV photon energy. The structures below 18 eV kinetic energy are due to shake-up satellites.

gases being mainly oxygen and carbon dioxide. Typical target pressures were of the order of 10^{-3} mbar in the interaction region, with the CMA and the detector at 10^{-6} mbar.

The measurements were performed at BESSY on the high energy TGM of the Fritz–Haber Institute[22] during two different beamtimes. The photon flux at the sample was approximately 10^{11} photons per second, and the combined monochromator/CMA resolution was typically 2 eV for the nitrogen and 3 eV for the oxygen 1*s* lines. All spectra were recorded to give peak intensities, integrated over all eight segments, of about 10 000 counts for the nitrogen 1*s* lines and 3000 counts for the oxygen 1*s* line. Figure 1 shows two typical raw spectra of the nitrogen 1*s* levels of N_2O, measured simultaneously on different anode segments at a photon energy of 436.3 eV. The collection time for such spectra was typically 15–30 min depending on ring current and monochromator throughput. The upper curve with higher 1*s* intensities was measured on a segment coincident with the polarization vector of the light, the other perpendicular to it. The different intensity ratios of the nitrogen lines directly reflect a difference in the β parameters. In this case, values of 0.77 and 1.64 are obtained for the β parameters of the N_C and the N_T lines, respectively. We note here that, in the particular case of near-threshold spectra, a scaled experimental secondary electron background has been subtracted. This background curve was obtained at one of the $1s$-3π resonances where no photoelectrons are created and only the smooth secondary electron background produced by the fast auger electrons is present. Due to the high count rates the accuracy of the cross sections and β parameters is not limited by counting statistics but by uncertainties in the calibration data[17–20] and by our method of background subtraction in this region. However, the statistical quality, as well as the stability of the operating conditions and of our methods of data analysis, can be estimated from the low scatter in the experimental partial cross section and β parameter curves shown in Figs. 2 and 4.

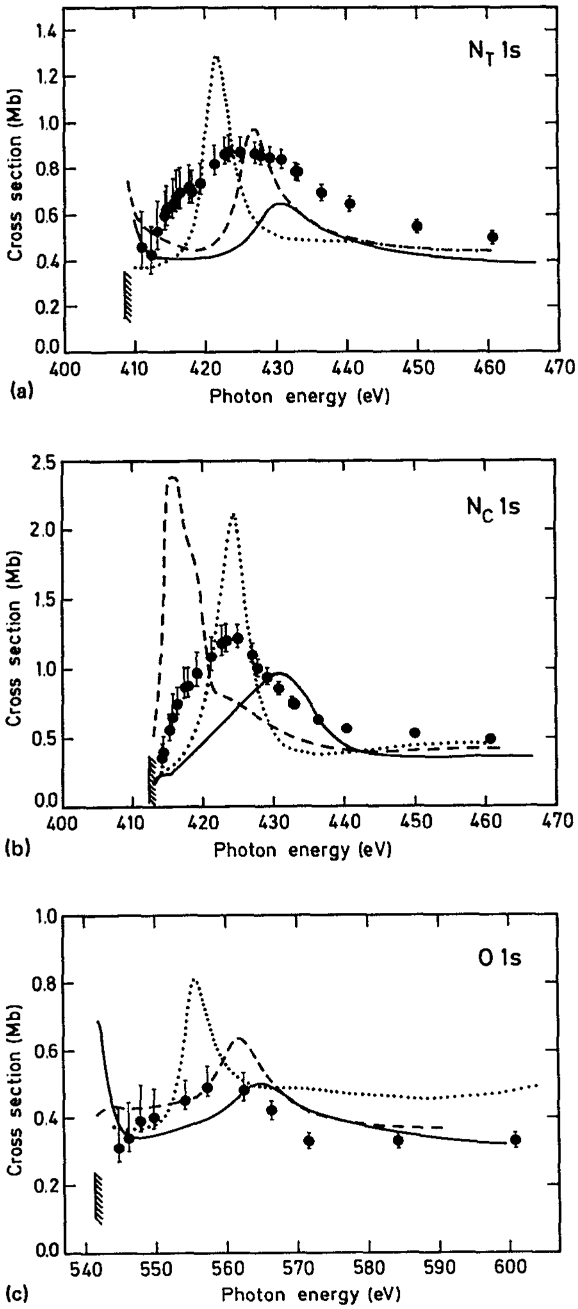

FIG. 2. Partial 1s single-hole photoionization cross sections of the N_T (a), N_C (b), and O (c) atoms of N_2O. The experimental points are scaled as described in the text. The error bars contain both statistical and systematic errors. Full lines represent RCHF, dashed lines FCHF results. The MSXα results of Ref. 7 are shown as dotted lines. The 1s ionization thresholds are indicated by hatched bars.

III. CALCULATIONS

The photoionization cross sections were calculated via the Schwinger variational method[23,24] using two different approximations for the static-exchange potential: the frozen-core Hartree–Fock (FCHF) approximation and the relaxed-core Hartree–Fock (RCHF) approximation. These methods have been described in detail elsewhere.[25,26] Briefly, the continuum photoelectron function is written as the partial-wave expansion,

TABLE I. Basis sets used in separable potential of Eq. (4).

Photoionization symmetry	Type of Gaussian function[a]	Exponents
σ	Cartesian s	16.0,8.0,4.0,2.0,1.0,0.5
	z	1.0,0.5
	Spherical $l=0$	2.0,1.0,0.5
	$l=1$	1.0,0.5
π	Cartesian x	8.0,4.0,2.0,1.0
	xz	1.0,0.5
	Spherical $l=1$	2.0,1.0,0.5
	$l=2$	1.0,0.5

[a]Cartesian functions are centered at the nuclei and the spherical functions on the central nitrogen atom. For details of the forms of these functions and their use, see Refs. 23 and 24.

$$\psi_{\mathbf{k}}^{(-)}(\mathbf{r})=\left(\frac{2}{\pi}\right)^{1/2}\sum_{lm}\frac{i^l}{k}\psi_{klm}^{(-)}(\mathbf{r})Y_{lm}^*(\hat{k}), \tag{1}$$

where each partial wave $\psi_{klm}^{(-)}$ satisfies its own Lippmann–Schwinger equation,

$$\psi_{klm}^{(-)}(\mathbf{r})=\phi_{klm}^{c}+G_c^{(-)}(\hat{v}+1/r)\psi_{klm}^{(-)}. \tag{2}$$

Here, $G_c^{(-)}$ is the Coulomb–Green's function with incoming wave boundary conditions, $\hat{v}$ is the static-exchange potential of the molecular ion, and ϕ_{klm}^{c} is the partial-wave Coulomb function. In the FCHF approximation $\hat{v}=\hat{v}^{FC}$ and the ion orbitals are taken to be the same as those of the neutral molecule. However, in the RCHF approximation $\hat{v}=\hat{v}^{RC}$ and the ion orbitals are taken from an SCF calculation for the fully relaxed molecular ion. In this approximation, the nonorthogonality of the photoelectron wave function leads to complications in the evaluation of the photoionization transition moment and in the derivation of the ion potential.[25] In K-shell ionization, however, these problems are not severe. The RCHF approximation has been shown to be superior to the FCHF approximation in that the former properly takes into account the screening of the nuclear charge brought about by electronic relaxation, an effect that can be profoundly important in regions of shape resonances.[25,26]

We proceed by assuming a separable approximation to the potential

$$\hat{V}=\hat{v}+1/r, \tag{3}$$

of the form

$$\hat{V}\simeq\hat{V}^s=\sum_{i,j}\langle\mathbf{r}|\hat{V}|\alpha_i\rangle(\mathbf{V}^{-1})_{ij}\langle\alpha_j|\hat{V}|\mathbf{r}\rangle, \tag{4}$$

where the set of functions $|\alpha_i\rangle$ are discrete basis functions, such as Cartesian–Gaussian functions, which have been shown to be quite effective in describing the inner region of the molecular ion potential.[23,24] The scattering basis sets used in the present calculations are specified in Table I. The solutions of the integral equations (2) can now be written as

$$\psi^{(-)}_{klm}(\mathbf{r}) = \phi^c_{klm}(\mathbf{r}) + \sum_{i,j} \langle \mathbf{r}|\, G_c^{(-)}\, \hat{V}\,|\alpha_i\rangle \times (\mathbf{D}^{-1})_{ij} \langle \alpha_j|\, \hat{V}\,|\phi^c_{klm}\rangle. \quad (5)$$

Here **V** and **D** denote matrices with elements

$$V_{ij} = \langle \alpha_i|\, \hat{V}\,|\alpha_j\rangle, \quad (6)$$

and

$$D_{ij} = \langle \alpha_i|\, \hat{V} - \hat{V} G_c^{(-)} \hat{V}\,|\alpha_j\rangle. \quad (7)$$

The electronic wave functions used in these studies were obtained with the [5*s*3*p*] contracted Gaussian basis set of Dunning[27] with additional 2*d* polarization functions.[28] This basis set gives an SCF energy of $-183.729\,404$ a.u. at the equilibrium geometry, $R_e(\mathrm{NN}) = 2.1273$ and $R_e(\mathrm{NO}) = 2.2418$ a.u. for the ground electronic state, $X\,^1\Sigma^+$. The energies of the relaxed $N_T(1s)$ hole, $N_C(1s)$ hole, and $O(1s)$ hole states are $-168.670\,876$, $-168.504\,243$, and $-163.844\,022$ a.u., respectively, with this basis. All matrix elements arising in the computation of the partial wave $\psi^{(-)}_{klm}$ are evaluated using single-center expansions about the central nitrogen atom. The details of these expansions are as follows:

(i) maximum angular momentum in the expansion of the occupied orbitals in the direct potential is 58.

(ii) maximum angular momentum in the expansion of the occupied orbitals in the exchange potential is 40 [1σ, $O(1s)$], 10 [2σ, $N_C(1s)$], 40 [3σ, $N_T(1s)$], 20 (4σ), 20 (5σ), 19 (6σ), 9 (7σ), 15 (1π), and 15 (2π).

(iii) maximum angular momentum in the expansion of $1/r_{12}$ in the direct and exchange terms is 116 and 58, respectively.

(iv) all other single-center expansions were truncated at $l = 58$.

The partial-wave expansion of the continuum orbital, Eq. (1), was truncated at $l = 8$ and the resulting radial integrals were obtained using a Simpson's rule quadrature. The grid contained 750 points and extended to 90.5 a.u. with a step size of 0.01 near the nuclei and a maximum step size of 0.4 a.u.

As discussed previously,[25] we write the spin-free transition amplitudes $I_{lm\mu}$ for the partial waves $\psi^{(-)}_{klm}$

$$I_{lm\mu} = \frac{1}{\sqrt{2}}(A^{(\mu)}_{1s\alpha,klm\beta} + A^{(\mu)}_{1s\beta,klm\alpha}) = \sqrt{2}\langle \bar{\Phi}^N_0|\Phi^N_0\rangle (\langle \psi^{(-)}_{klm}|r_\mu|\phi_{1s}\rangle - \sum_{r,r'} \langle \psi^{(-)}_{klm}|\phi_r\rangle (\mathbf{S}^{-1})_{rr'} \langle \psi_{r'}|r_\mu|\phi_{1s}\rangle). \quad (8)$$

Here $r_{\pm 1}$ corresponds to $\mp (x \pm iy)/\sqrt{2}$ and r_0 to z. The orbital ϕ_{1s} refers to the particular core orbital which is being ionized and **S** represents the overlap matrix of spatially relaxed–frozen-core orbitals $\langle \psi_r|\phi_{r'}\rangle$. The N-electron relaxed–frozen overlap, $\langle \bar{\Phi}^N_0|\Phi^N_0\rangle$, is given by the square of det(**S**). The decomposition of the full amplitude into direct $I^{(\mathrm{I})}$ and conjugate $\mathrm{I}^{(\mathrm{II})}$ contributions,

$$I_{lm\mu} = I^{(\mathrm{I})}_{lm\mu} + I^{(\mathrm{II})}_{lm\mu}, \quad (9)$$

according to Eq. (8), is obvious. In the FCHF approximation, the N-electron overlap is equal to unity and the only nonvanishing contribution to the amplitude comes from the direct part. In the RCHF approximation, the N-electron overlap is generally not unity. The square of this quantity is the so-called spectroscopic factor; its deviation from unity gives the relative intensity of shake-up and shake-off excitations. The values of the spectroscopic factors obtained here are 0.736 for the $N_T(1s$ hole) state, 0.768 for the $N_C(1s$ hole) state, and 0.731 for the $O(1s$ hole) state. These compare with values of 0.569, 0.624, and 0.584, respectively, from a Green's function study.[29] In addition, both the direct and conjugate part contribute to the amplitude in the RCHF approximation. Indeed, the energy dependence of the conjugate part gives a measure of the sensitivity of the photoelectron wave function to the effect of electronic relaxation of the ionic core. In addition, these conjugate amplitudes are extremely important in studying cross sections due to satellite states,[30] and have been analyzed in some detail in our original study on CO photoionization.[25] The calculated amplitudes of Eq. (8) are related to the total cross section by (in a.u.)

$$\sigma = \frac{4\pi^2}{3c} Ek \sum_{lm\mu} |I_{lm\mu}|^2, \quad (10)$$

where E is the photon energy, c is the speed of light, and $k^2/2$ is the photoelectron kinetic energy.

IV. RESULTS AND DISCUSSION

The N_T, N_C, and O 1*s* partial photoionization cross sections determined from our angle-resolved photoelectron spectra are shown in Figs. 2(a)–2(c), along with the results of MSXα calculations of Grimm *et al.*[7] and of the FCHF and RCHF calculations described in Sec. III. The experimental points have been scaled to the total absorption cross sections[31] at 500 and 600 eV photon energy for nitrogen and oxygen, respectively. The total cross sections have been corrected for valence, but not for shake-up and shake-off contributions. Since the spectroscopic factors are in the range of ~ 0.6 (see Green's function values of Sec. III), the experimental partial cross sections shown in Figs. 2(a)–2(c) are overestimated by approximately 40%. All experimental curves show broad resonance peaks located at approximately 424 eV photon energy for both N_T and N_C ionization and at 558 eV for O 1*s* ionization. On a kinetic energy scale the resonance positions are 15.5, 11.5, and 17 eV for N_T, N_C, and O 1*s* ionization, respectively. The strongest resonance peak together with the narrowest width is observed for the N_C atom while the weakest structure appears in the O 1*s* spectrum. The positions and profiles of these resonance peaks indicate a clear dependence on the specific ionization site. In contrast, core level transitions to the unoccupied, bound molecular states differ by not more than 1 eV:[12] The differences between the N_T, N_C, and O 1*s* ionization energies and the energies necessary to excite the 1*s* electrons into the empty 3π orbital are 7.4, 7.8, and 6.6 eV, respectively. Examination of the energy dependence of the RCHF eigenphase sums, on the other hand,

shows that the maximum rise in these quantities, indicative of resonant behavior, occurs at nearly the same photoelectron energy for all of the core holes. This suggests that the resonant continuum wave functions associated with these holes have a similar character, but that the resonance profiles of the cross sections differ because the target K-shell orbital probes a different spatial part of the continuum orbital in the photoelectron matrix element. Vibrationally resolved calculations and studies which examine the electronic charge distribution of the continuum wave function near the ion core would be helpful in clarifying these ideas.

As is well known from many other examples, the cross sections calculated with the MSXα method[7] are generally too narrow and overestimate the magnitude of shape resonance features. However, the peak positions agree very well with the experimental results, particularly for N_C and O 1s ionization. For N_T, the calculated resonance position is shifted to lower energy by 2 to 3 eV. However, there still remains a 1.5 eV difference in photoelectron energy between the MSXα results for the N_T and the N_C shape resonance positions and the measured values which the authors attribute to relaxation effects.[7] In their method relaxation is indirectly accounted for by adjusting the net charge on the individual atoms. In contrast, calculations based on HF methods can gauge the magnitude of relaxation by determining the continuum final state using relaxed core orbitals vs frozen core orbitals. In this regard, we note the different behavior of the shape resonance at each atomic site when relaxation is included within the HF model. For the central nitrogen atom, the FCHF resonance position is about 8 eV lower than the experimental value, and the RCHF result is 6 eV higher. A similar but smaller energy shift is observed for the σ shape resonance in CO.[25] In contrast, for the terminal atoms, N_T and O, there is a very small energy shift between the FCHF and RCHF results for the shape resonance position and, in addition, the resonance positions are significantly higher in energy relative to the MSXα results. In this instance therefore the position of the shape resonance is much more sensitive to relaxation upon removal of a 1s electron from the central nitrogen atom than from the terminal atoms. Interestingly, all RCHF results are 6 to 7 eV higher than the experimental values, no matter which atom is ionized. Furthermore, a closer inspection of the cross section ratio $\sigma(N_C)/\sigma(N_T)$ (Fig. 3) reveals that, except for an energy shift, the relative behavior of these cross sections is very well reproduced by the RCHF calculations, suggesting that the RCHF method includes relaxation effects correctly. The shift to higher energy is typical of this method and is attributed to the neglect of target polarization.[25]

For both the terminal nitrogen and the oxygen atom the RCHF calculations predict a steep increase of the partial cross sections directly at threshold, in contrast to the experimentally determined values. Moreover, the RCHF $k\sigma$ eigenphase sums (not shown) show two distinct rises indicative of resonant behavior, one near threshold and one 10–20 eV higher in energy. This behavior is reminiscent of the two shape resonances, but somewhat shifted in energy, as seen in valence shell ionization.[2–6] Unfortunately, our

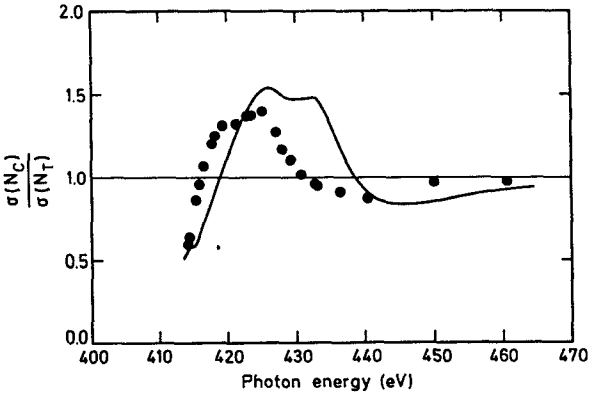

FIG. 3. Ratio of the N_C and the N_T partial cross sections, $\sigma(N_C)/\sigma(N_T)$. Points: experiment; full line: RCHF theory.

experimental data do not extend down to threshold, and, in addition, the two points at lowest energies in all the experimental curves shown have larger error bars. Indeed, other experimental techniques such as electron-energy-loss spectroscopy (EELS) and zero-kinetic-energy (ZEKE) photoelectron spectroscopy are also limited in interpreting this low energy region. For example, the ZEKE measurements of Habenicht et al.[32] show that the N_T 1s ionization cross section at threshold is about twice as large as for N_C ionization, in agreement with the trend observed in Fig. 3, but the results are not given on an absolute scale. As a first approximation, one can rescale these relative measurements to an absolute scale by combining them with the total photoabsorption cross section curve obtained from EELS[12] and with our present data. However, one cannot justify extrapolating to threshold since an unknown fraction of transitions to other states, such as Rydberg orbitals belonging to the N_C atom, are superimposed on the N_T 1s continuum. The same holds, in principle, for O 1s ionization. In this case, however, the total photoabsorption cross section increases strongly at threshold. This could certainly be taken as a strong indication of the *presence of another resonance very near the O 1s ionization threshold*, corresponding to the one observed in the valence level photoionization studies.[4–6] It is also instructive to compare with the core level ionization of the isoelectronic linear molecule CO_2.[8] Here, a resonance in the continuum, associated with the $4\sigma_u(\sigma^*)$ molecular orbital, is present in the C 1s ionization cross section around 14 eV above the ionization threshold. In the O 1s cross section, this same resonance is apparent at a slightly higher electron energy (17 eV), and in addition there is clear evidence of a second resonance at threshold due to the $5\sigma_g(\sigma^*)$ orbital. For symmetry reasons, this latter state is not accessible from the $2\sigma_g$ C 1s orbital. The similarity with N_2O is remarkable, even though the inversion symmetry is broken in nitrous oxide.

Our measured values for the asymmetry parameter β, along with those of theory, are shown in Figs. 4(a)–(c). Note the remarkably different behavior for the central nitrogen atom on the one hand, and the two terminal atoms, N_T and O on the other. For the N_C atom a broad oscillation is observed with a maximum at 423 eV and a mini-

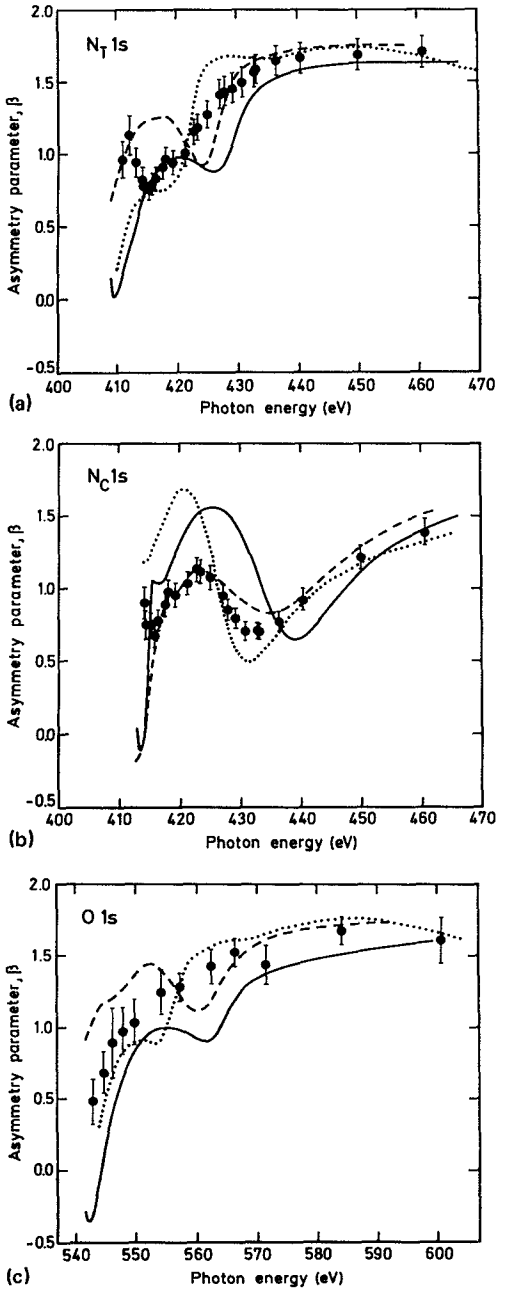

FIG. 4. Asymmetry parameters, β, for 1s single-hole photoionization of the N_T (a), N_C (b), and O (c) atoms of N_2O. As in Fig. 2, the experimental results are shown as points, the RCHF and FCHF results as full and dashed lines, respectively, and the MSXα results of Ref. 7 as dotted lines. The error bars on the experimental points contain both statistical and systematic errors.

mum at 433 eV. The two data points at lowest energy are too uncertain to clearly identify a second minimum at 415 eV, seen in the calculated values. The overall shape of the β parameter curve is well reproduced by the MSXα and HF calculations although there are marked deviations from the experimental values both in the energy positions of the structures and in the overall magnitude of the oscillation around 423 eV, particularly in the MSXα and RCHF results. Compared with C 1s ionization of CO_2, we note again a remarkable similarity.[17] For the N_T atom we find the β parameter steeply decreasing towards threshold with a narrow minimum at 415 eV. Both the FCHF and RCHF calculations are in broad agreement but place the minimum at much higher energy. The overall appearance of the O 1s β parameter is very similar, but in contrast to the N_T case, no minimum near threshold is seen experimentally. In order to understand the striking difference between the terminal nitrogen and oxygen and the central nitrogen β curves, we should consider the following factors: (i) the different environment of the excited atoms can introduce a change in the angular distribution,[7] (ii) the influence of a shape resonance on the β parameter extends over a much larger energy range than the separation of the two resonances, presumably present in this case and suggesting that interference effects could be possible and, (iii) the lower energy resonance at threshold could dominate the behavior of the terminal atoms and prevent another pronounced minimum in the vicinity of the upper resonance to form.

V. CONCLUSION

We have presented the results of experimental and theoretical studies of angle-resolved photoelectron spectra of the core levels of nitrous oxide. The measured and calculated cross sections and β parameters show site-specific behavior in the sense that the central nitrogen atom behaves differently from the terminal atoms. In addition, it is quite interesting that the peak of the shape resonance occurs at different photoelectron energies for N_T and N_C ionization, whereas the transitions to the unoccupied 3π orbital occur at the same energy. Examination of the RCHF eigenphase sums suggests that, in fact, the shape resonant photoelectron orbitals for the core holes are similar in character but that these (1s) target orbitals probe different spatial parts of the "resonance" wave function in the photoelectron matrix element. This is consistent with the interpretation of the vibrationally resolved studies of the near-threshold resonance in the 7σ valence ionization[4–6] where the resonant continuum state was seen to extend over the entire molecule and not to be localized between either the N–N or the N–O atoms.

The experimental data do not give a conclusive answer about the behavior within the region 5 eV above threshold where the RCHF method predicts a steep increase in the N_T and O 1s ionization cross section. However, there are clear indications of the presence of an additional shape resonance based on the following considerations: (i) there is a strong enhancement in the O 1s total photoabsorption cross section at threshold, (ii) it is unlikely that the resonance would be shifted about 10 eV to higher energies in going from valence to core ionization. The energy position can be expected to shift a few eV in the opposite direction.[1] This shift, in fact, identifies the near-threshold core ionization shape resonance with the strong shape resonance seen in 7σ ionization 3–4 eV above threshold; and (iii), there are close similarities in core ionization of CO_2. In this respect it would certainly be interesting to carefully investigate the core levels of the series CO_2, OCS, and CS_2 and, of course, N_2O, directly at, and within the first few eV, above

threshold. Vibrationally resolved studies will be helpful in examining the possible existence of a shape resonance near threshold.

ACKNOWLEDGMENT

We gratefully acknowledge the help of V. Schmidt who generously allowed us to extensively modify his magic angle CMA. This work has been supported by the Bundesminister für Forschung und Technologie, Project 05 490FXB/TPl and by the National Science Foundation (CHE-8521391). We also acknowledge use of resources of the San Diego Supercomputer Center which is supported by the National Science Foundation.

[1] See, for example, J. L. Dehmer, A. C. Parr, and S. H. Southworth, in *Handbook on Synchrotron Radiation*, Vol. II, edited by G. V. Marr (North-Holland, Amsterdam, 1987).
[2] T. A. Carlson, P. R. Keller, J. W. Taylor, T. Whitley, and F. A. Grimm, J. Chem. Phys. **79**, 97 (1983).
[3] M. Braunstein and V. McKoy, J. Chem. Phys. **87**, 224 (1987).
[4] M. Braunstein and V. McKoy, J. Chem. Phys. **90**, 1535 (1989).
[5] L. A. Kelly, L. M. Duffy, B. Space, E. D. Poliakoff, P. Roy, S. H. Southworth, and G. M. White, J. Chem. Phys. **90**, 1544 (1989).
[6] T. A. Ferrett, A. C. Parr, S. H. Southworth, J. E. Hardis, and J. L. Dehmer, J. Chem. Phys. **90**, 1551 (1989).
[7] F. A. Grimm, T. A. Carlson, J. Jiménez-Mier, B. Yates, J. W. Taylor, and B. P. Pullen, J. Electron Spectrosc. Relat. Phenom. **47**, 257 (1988).
[8] N. Padial, G. Csanak, B. V. McKoy, and P. W. Langhoff, Phys. Rev. A **23**, 218 (1981).
[9] J. L. Dehmer, A. C. Parr, S. Wallace, and D. Dill, Phys. Rev. A **26**, 3283 (1982).
[10] J. L. Dehmer, A. C. Parr, S. H. Southworth, and D. M. P. Holland, Phys. Rev. A **30**, 1783 (1984).
[11] D. L. Lynch, S. N. Dixit, and V. McKoy, J. Chem. Phys. **84**, 5504 (1986).
[12] G. R. Wight and C. E. Brion, J. Electron Spectrosc. Relat. Phenom. **3**, 191 (1974).
[13] A. Bianconi, H. Petersen, F. C. Brown, and R. Z. Bachrach, Phys. Rev. A **17**, 1907 (1978).
[14] K. Siegbahn, C. Nordling, G. Johansson, J. Hedman, P. F. Heden, K. Hamrin, U. Gelius, T. Bergmark, L. O. Werme, R. Manne, and Y. Baer, *ESCA Applied to Free Molecules,* (North-Holland, Amsterdam, 1969).
[15] V. Schmidt, Phys. Lett. A **45**, 63 (1973); J. A. R. Samson and A. F. Starace, J. Phys. B **8**, 1806 (1975).
[16] J. Feldhaus, A. L. D. Kilcoyne, K. J. Randall, M. Schmidbauer, and W. Erlebach (to be published).
[17] C. M. Truesdale, D. W. Lindle, P. H. Kobrin, U. E. Becker, H. G. Kerkhoff, P. A. Heimann, T. A. Ferrett, and D. A. Shirley, J. Chem. Phys. **80**, 2319 (1984).
[18] R. B. Kay, P. E. Van der Leeuw, and M. J. Van der Wiel, J. Phys. B **10**, 2513 (1977).
[19] D. W. Lindle, L. J. Medhurst, T. A. Ferrett, P. A. Heimann, M. N. Piancastelli, S. H. Liu, D. A. Shirley, T. A. Carlson, P. C. Deshmukh, G. Nasreen, and S. T. Manson, Phys. Rev. A **38**, 2371 (1988).
[20] U. Becker (private communication).
[21] F. Wuilleumier, Adv. X-Ray Anal. **16**, 63 (1973).
[22] E. Dietz, W. Braun, A. M. Bradshaw, and R. L. Johnson, Nucl. Instrum. Methods Phys. Res. A **239**, 359 (1985).
[23] R. R. Lucchese, G. Raseev, and V. McKoy, Phys. Rev. A **25**, 2572 (1982).
[24] R. R. Lucchese, K. Takatsuka, and V. McKoy, Phys. Rep. **131**, 147 (1986).
[25] J. Schirmer, M. Braunstein, and V. McKoy, Phys. Rev. A **41**, 283 (1990).
[26] D. L. Lynch and V. McKoy, Phys. Rev. A **30**, 1568 (1984).
[27] T. H. Dunning, J. Chem. Phys. **53**, 2823 (1971).
[28] J. Andzelm, M. Koblukowski, E. Radzio-Andzelm, Y. Sakai, and H. Tatewaki, in *Gaussian Basis Sets for Molecular Calculations*, edited by S. Huzinaga (Elsevier, Amsterdam, 1984), p.23.
[29] J. Schirmer (private communication).
[30] J. Schirmer, M. Braunstein, and V. McKoy, J. Chem. Phys. (submitted).
[31] D. M. Barrus, R. L. Blake, A. J. Burek, K. C. Chambers, and A. L. Pregenzer, Phys. Rev. A **20**, 1045 (1979).
[32] W. Habenicht, H. Baiter, K. Müller-Dethlefs, and E. W. Schlag, Phys. Scripta **41**, 814 (1990).